An Analytical Study of Heat Transfer in Laminar-Turbulent Transition Flow Between Parallel Plates

WILLIAM N. GILL and SHAW MEI LEE

Syracuse University, Syracuse, New York

With the results of a modification of Prandtl's mixing length theory, heat transfer in laminar-turbulent transition flow is considered. An analytical study was made to obtain the eigenvalues, Nusselt numbers, and temperature distribution for transition region flows between constant temperature parallel plates. Reynolds numbers ranging from 4,800 to 43,000 and Prandtl numbers from 0.01 to 100 were investigated. Six to nine eigenvalues were obtained for each set of parameters. These values were used to compute local Nusselt numbers and thermal entrance lengths. The practicality of four numerical methods used for solving the associated Sturm-Liouville system is discussed.

It is shown how heat transfer effects change in the transition region. As expected, these changes are more rapid for higher N_{Pr} fluids where eddy diffusion is most effective.

This analytical investigation represents an attempt to explore heat transfer in the transition region for fluid flowing between infinite parallel plates. Many investigations considering heat transfer for laminar or turbulent flows are available. However the transition region between these flow regimes is relatively unexplored.

For the laminar-flow problem variations on the Graetz solution are numerous. Significant fully developed convection heat transfer calculations have been made for turbulent flow by Reynolds (*18*), Taylor (*24*), Prandtl (*16*), Murphree (*14*), Von Kármán (*27*), Reichardt (*17*), Martinelli (*11*), Lin, Moulton, and Putnam (*10*), Seban and Shimazaki (*20*), Deissler (*4, 5*), Sleicher (*22*), Sparrow, Hallman, and Siegel (*23*), and others. However the investigation of the transition region has been hindered by a lack of an adequate expression for the velocity distribution. This investigation utilized the velocity and eddy diffusivity distributions given by Gill and Scher (*8*) to solve the energy equation.

ANALYSIS

This investigation employs the following assumptions:

1. Velocity profile is fully developed.
2. Uniform entrance temperature.
3. Constant fluid properties and wall temperature.
4. Ratio of eddy diffusivity of momentum and heat is constant and equal to one. For low N_{Pe} flows this assumption appears to be tenuous. However to indicate trends in the transition region over a wide range of N_{Pr} calculations for $N_{Pr} = 0.01$ have been included.
5. The wall is smooth.
6. The velocity and temperature fields are symmetrical.
7. Axial conduction is neglected. This assumption will be shown to introduce negligible errors.

The energy equation for fully developed flow between infinite parallel plates neglecting source terms is

$$u\frac{\partial T}{\partial x} = \frac{\partial}{\partial r}\left[(\alpha + \epsilon_h)\frac{\partial T}{\partial r}\right] \quad (1)$$

If $\left(1 + \frac{\epsilon_h}{\nu}N_{Pr}\right)$ is denoted by f, Equation (1) becomes in dimensionless form

$$U N_{Pe_m}\frac{\partial \theta}{\partial \beta} = \frac{\partial}{\partial \epsilon}\left(f\frac{\partial \theta}{\partial \epsilon}\right) \quad (2)$$

Assuming

$$\theta = \sum_n A_n X_n(\beta)\, Y_n(\epsilon)$$

then one gets

$$\frac{dX_n}{d\beta} + \frac{\lambda_n}{N_{Pe_m}}X_n = 0 \quad (3)$$

$$\frac{d}{d\epsilon}\left(f\frac{dY_n}{d\epsilon}\right) + \lambda_n U Y_n = 0 \quad (4)$$

and the solution to Equation (1) is

$$\theta = \sum_{n=1}^{\infty} A_n e^{-\frac{\lambda_n \beta}{N_{Pe_m}}} Y_n(\epsilon) \quad (5)$$

where Y_n and λ_n are eigenfunctions and eigenvalues associated with Equation (4).

The boundary conditions in view of assumptions 2, 3, and 6 are

$$\theta(0, \epsilon) = 1 \text{ or } \sum_{n=1}^{\infty} A_n Y_n(\epsilon) = 1 \quad (5a)$$

$$\theta(\beta, 1) = 0 \text{ or } Y_n(1) = 0 \quad (5b)$$

$$\frac{\partial \theta(\beta, 0)}{\partial \epsilon} = 0 \text{ or } \frac{dY_n(0)}{d\epsilon} = 0 \quad (5c)$$

Since Equations (4), (5*b*), and (5*c*) constitute a Sturm-Liouville system

$$A_n = \frac{\int_0^1 U Y_n\, d\epsilon}{\int_0^1 U Y_n^2\, d\epsilon} \quad (6)$$

Alternately

$$A_n = \frac{-1}{\lambda_n \dfrac{dY_n(1)}{d\lambda_n}} \quad (7)$$

The temperature gradient at the wall is readily obtained by taking the derivative of Equation (5)

$$\frac{\partial\theta(\beta,1)}{\partial\epsilon}=\sum_{n=1}^{\infty}A_n e^{-\frac{\lambda_n\beta}{N_{Pe_m}}}\frac{dY_n(1)}{d\epsilon} \tag{8}$$

and the bulk mean temperature is by definition

$$\theta_b=\frac{\int_o^1 U\,\theta\,d\epsilon}{\int_o^1 U\,d\epsilon}$$

Using Equation (4) one obtains

$$\theta_b=\frac{u_m}{u_b}\sum_{n=1}^{\infty}A_n e^{-\frac{\lambda_n\beta}{N_{Pe_m}}}\left(-\frac{1}{\lambda_n}\right)\frac{dY_n(1)}{d\epsilon} \tag{9}$$

By definition

$$N_{Nu}=\frac{4\,h\,r_o}{K}$$

which yields, with Equations (8) and (9)

$$N_{Nu}=\frac{4u_b\sum_{n=1}^{\infty}A_n e^{-\frac{\lambda_n\beta}{N_{Pe_m}}}\frac{dy_n(1)}{d\epsilon}}{u_m\sum_{n=1}^{\infty}A_n e^{-\frac{\lambda_n\beta}{N_{Pe_m}}}\left(\frac{1}{\lambda_n}\right)\frac{dy_n(1)}{d\epsilon}} \tag{10}$$

As β approaches infinity, the asymptotic Nusselt number is obtained as

$$N_{Nu_\infty}=\frac{4\,U_b\,\lambda_1}{U_m} \tag{11}$$

The velocity distribution and eddy diffusivity of momentum equations were taken from Gill and Scher (8). Hence

$$u^+=\int_o^{y^+}\frac{2d}{1+\sqrt{1+4cd}}\,dy^+ \tag{12}$$

$$\frac{\epsilon_m}{\nu}=\frac{-1+\sqrt{1+4cd}}{2} \tag{13}$$

where

$$c=k^2\,y^{+2}\left[1-e^{-\phi\frac{y^+}{y^+_m}}\right]^2$$

$$d=1-\frac{y^+}{y^+_m}$$

$$\phi=\frac{y^+_m-60}{22}$$

Equations (12) and (13) together with

$$u^+_b=\frac{\int_o^{y^+_m}u^+\,dy^+}{y^+_m} \tag{14}$$

$$N_{Re}=4\,u^+_b\,y^+_m \tag{15}$$

$$F=\frac{32\,y_m{}^{+2}}{N^2_{Re}} \tag{16}$$

enable one to calculate the desired heat transfer results.

METHODS OF COMPUTATIONS

Direct numerical integration of Equation (12) with the Newton-Cotes formulas gave the velocity distribution data. The eddy diffusivity was computed at the same time.

Several methods for obtaining the eigenvalues and eigenfunctions of Equation (4) were employed. The smallest eigenvalue may be determined easily with the Stodola-Vianello iteration technique, but even when refinements described by Beskin and Rosenberg (2) were used, the method was not found to be satisfactory for determining higher-order eigenvalues. The accuracy gradually decreases because of the sweeping process required for each higher-mode eigenvalues.

When one follows Beckers (1), a power series expansion in λ_n

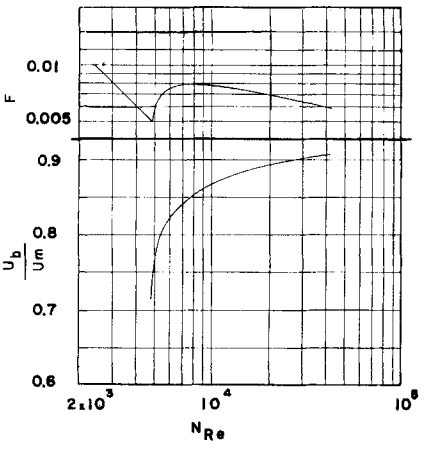

Fig. 1. Friction factor and velocity ratio vs. N_{Re}.

$$Y_n(\epsilon)=\sum_{l=0}^{\infty}\Psi_l(\epsilon)\,\lambda^l{}_n$$

can also be used. Only the first two or three eigenvalues were obtained satisfactorily by this method because of accumulated error inherent in the successive numerical integration in the evaluation of series coefficients and increased truncation error for larger eigenvalues.

It is recommended that Ritz's variational method (25) should be used for the first two or three eigenvalues and then direct numerical integration to obtain higher order eigenvalues. In the latter case several trials are necessary so that the eigenvalue finally used yields the correct boundary values at $\epsilon = 1$. The chief advantage of this method is that the determination of λ_{n+1} is not dependent on the accuracy of λ_n, and hence error does not accumulate.

For convenience Equation (4) was transformed to the form

$$\frac{d^2Y_n}{d\sigma^2}+\lambda_n\,U\,f\,Y_n=0$$

by the transformation

$$\sigma=\int_o^{\epsilon}\frac{d\epsilon}{f}$$

In this form $df/d\epsilon$ is not required, and the coefficients in this equation are multiplied by f rather than divided by f. For N_{Pr} greater than 1 it was found desirable to express f in the form $\left(\frac{1}{Pr}+\frac{\epsilon_h}{\nu}\right)$. The conversion of necessary quantities accompanying this form of f is easily achieved.

Using

$$Z_n=\frac{dY_n}{d\sigma}$$

one may reduce the second-order differential equation to

$$\frac{dY_n}{d\sigma}=Z_n$$

$$\frac{dZ_n}{d\sigma}=-\lambda_n\,U\,f\,Y_n$$

In this way the differential Equation (4) was solved directly with the Runge-Kutta formulas. The boundary conditions are

$$Z_n=0 \text{ at } \epsilon=0$$

$$Y_n=0 \text{ at } \epsilon=1$$

and Y_n may be taken equal to one at the center of the channel without loss of generality. Since

$$f=1 \text{ at } \epsilon=1$$

the derivatives $(dY_n/d\epsilon)_{\epsilon=1}$ and $(dY_n/d\lambda_n)_{\epsilon=1}$ are evaluated at the same time. The false position method was used for testing and generating better eigenvalues for successive trials.

With the quantities mentioned above available, it is a straightforward computation to obtain A_n, the temperature distribution, and Nusselt number. Conventionally thermal entrance lengths were determined as the lengths at which the ratios of local to asymptotic Nusselt numbers were 1.05.

RESULTS AND DISCUSSION

Since they were not previously given, the ratio of average to maximum velocity and the friction factor vs. N_{Re} relation based on Equations (14) and (16) are shown in Figure 1.

Some comments concerning these seem in order. Qualitatively the results correspond well with the experimental data of Whan and Rothfus (28) and Rothfus and Baldwin (19). However these investigators suggest that transi-

TABLE 1. EIGENVALUES

N_{Re}			42,647			
N_{Pr}	100	10	1	0.1	0.01	
λ_1	196.5	92.49	32.45	9.184	3.54	
λ_2	72,280	7,620	897.8	132.1	36.62	
λ_3	225,900	23,890	2,716	379.6	102.9	
λ_4	434,600	48,000	5,441	750.9	202.5	
N_{Re}			11,695			
N_{Pr}	100	10	1	0.1	0.01	
λ_1	56.71	27.71	11.34	4.547	2.82	
λ_2	20,890	2,306	297.7	58.71	28.08	
λ_3	55,370	6,558	854	166.5	79.37	
λ_4	95,400	12,600	1,676	328.1	157	
N_{Re}			5,763			
N_{Pr}	100	10	1	0.1	0.01	
λ_1	20.48	10.71	5.322	3.106	2.641	
λ_2	5,280	675.6	109.7	35.89	26.6	
λ_3	11,210	1,795	313.3	102.8	76.46	
λ_4	21,010	3,331	614.8	205	152.8	
N_{Re}			5,038			4,800
N_{Pr}	100	10	1	0.1	0.01	
λ_1	11.56	6.303	3.666	2.815	2.684	2.828
λ_2	1,535	247.9	58.78	31.63	28.46	32.15
λ_3	3,516	653.4	166.1	91.46	82.67	93.48
λ_4	6,708	1,260	327.2	182.5	165.3	186.8

tion between plates occurs at $N_{Re} = 2{,}750$, whereas the transition point used here is $N_{Re} = 4{,}800$. If in the original development of Equations (12) and (13) the critical N_{Re} for tubes has been taken as 1,200 as suggested (*28*), rather than 1,800 on the basis of Senecal's results (*21*), the authors' critical N_{Re} for plates would be 3,200. On the other hand stability theory (*12*) predicts considerably higher N_{Re} critical, and the velocity distribution used here agrees well with other experimental data in the transition region (*8*). Also, since so many factors including heat transfer affect the laminar turbulent transition, it does not seem that a definite answer is available yet. Therefore this work may be considered an attempt to describe analytically how the transition to turbulent flow affects heat transfer, even though the transition region may shift with respect to N_{Re}, depending on the experimental conditions.

Some of the calculated eigenvalues are tabulated in Table 1.* These values will vary somewhat depending on the physical assumptions made. It is seen that the change in the magnitude of the eigenvalues is abrupt for the lower modes. For those wishing to make calculations at conditions other than those investigated here, log-log cross plots of the λ_n for various values of the parameters should be very useful.

It is well known that the N_{Nu} dependence on the number of eigenvalues used is most important in the entrance region, and that the number of eigenvalues necessary for computing accurate values of local Nusselt numbers depends strongly on the distance from the entrance. For $\beta \geq 3$, three to eight eigenvalues will be sufficient depending on N_{Re} and N_{Pr}. In the transition region the number of eigenvalues necessary is not simply related to N_{Pe} as in the Graetz problem. For $N_{Pr} \geq 1$, the number of eigenvalues necessary is less for higher N_{Re} and smaller N_{Pr}. However as N_{Re} increases, the dependence on N_{Re} decreases; Also as N_{Pr} decreases, the N_{Re} effect decreases and shows a slight tendency toward requiring fewer eigenvalues for smaller N_{Re}.

The coefficients A_n were calculated with both Equations (6) and (7). For lower N_{Re} and N_{Pr} the agreement between these two equations was better than for higher values of these parameters. For the laminar flow case the results were in good agreement with Brown's triple precision calculation (*3*). The first four coefficients are tabulated in Table 2. At higher N_{Re} and N_{Pr}, because of the drastic change in the eigenfunctions near the wall, care must be taken in using Equation (6). Equation (7) was found to be more satisfactory for this case. Table 3 gives the corresponding derivatives of the eigenfunctions at the wall.

Figures 2*a*, 2*b*, 2*c*, and 2*d* show the local N_{Nu} and thermal entrance lengths. Calculated thermal entrance lengths reported in the literature (*1, 4, 22, 23*) differ significantly depending on the boundary condition at the wall, the method used, and the number of eigenvalues determined. It was found that the thermal entrance length for high Prandtl number fluids changes rapidly in the transition region and shows a drastic decrease as N_{Re} increases. This occurs because of increased eddy diffusion which moves the effective thermal region closer to the wall. Thus, in the fully developed turbulent region, the temperature profile across the channel becomes very flat and the temperature gradient at the wall very large, so that it requires only a short distance for the fluid to establish this kind of profile (*4*). For low Prandtl number fluids, except at the beginning of the transition region, the thermal entrance length increases with N_{Re}. In this case the increase in total radial diffusion is not sufficient to offset the improved axial convection. Hence a longer distance is required to approach the asymptotic profile. If one plots the thermal entrance lengths for various values of the parameters, some interesting results are obtained. With $N_{Pr} \geq 1$, the thermal entrance length decreases with increasing N_{Re}, and for $N_{Pr} = 0.01$ it increases with increasing N_{Re}. The behavior of $N_{Pr} = 0.1$ is particularly interesting. It is seen that a minimum occurs with increasing N_{Re}, and this is apparently the region in which the dominant transport mechanism changes with regard to establishing the temperature field. That is at the start of the transition region eddy diffusion more than compensates for the increased axial convection, but as N_{Re} increases further, axial convection predominates.

Asymptotic N_{Nu} calculated by Equation (11) are presented in Figure 3. For high N_{Pr}, N_{Nu} increases very rapidly as N_{Re} changes from 4,800 to 5,038. The asymptotic results also have been compared with other investigations. Poppendiek's (*15*) low N_{Pr} results are higher but give better agreement at larger values of N_{Re}. However the difference increases as N_{Re} decreases. Agreement with Gill and Scher's (*6*) results for $N_{Pr} \geq 1$ is

* Complete tables of λ_n, A_n, and $\frac{dy_n(1)}{d\epsilon}$ have been deposited as document 7075 with the American Documentation Institute, Photoduplication Service, Library of Congress, Washington 25, D. C., and may be obtained for $1.25 for photoprints or for 35-mm. microfilm.

good for $N_{Re} \geq 10{,}000$, but their results are lower in the low N_{Pr} range. These differences apparently are due to the velocity distributions used. However the low N_{Pe} calculations may be in error on the order of 10% or more because of the uncertainty in the ratio ϵ_h/ϵ_m. Also body force or natural convection effects are more important in low N_{Re} flows and introduce error as well. The problem involving the magnitude of the eddy diffusivity ratio may in large measure be avoided by considering that N_{Pr} referred to here is really $\left(\frac{\epsilon_h}{\epsilon_m} N_{Pr}\right)$.

Since many eigenvalues are necessary in order to compute N_{Nu} at very small values of β, it is much simpler to calculate N_{Nu} by the following asymptotic equation:

$$N_{Nu} = 1.076 \left[\frac{N_{Pr} N_{Re}^2 F}{4\beta}\right]^{1/3} \qquad (17)$$

This equation is essentially the Lévêque approximation and may easily be derived from a result given elsewhere (*13*). The length at which both methods give approximately the same value of N_{Nu} depends on the parameters. This length decreases as N_{Re} increases or as N_{Pr} decreases. The results indicate N_{Nu} calculated with Equation (17) is reasonably good up to substantial distances from the inlet for $N_{Pr} > 1$. On the other hand, at low N_{Pr}, Equation (17) is restricted to distances of $\beta \leq 1$. A better asymptotic approximation for low N_{Pr} and $N_{Re} > 10{,}000$ can probably be obtained without difficulty by neglecting eddy diffusion and using a velocity distribution in the form

$$u^+ = y^+ + a\,y^{+2} + \ldots$$

which will describe the velocity at greater distances from the wall, together with a method similar to that given in (7). However boundary layer types of approximations for liquid metal heat transfer can probably not be expected to apply well much beyond $\beta \leq 1$, since θ_b varies rapidly with β for low N_{Pr} fluids.

TABLE 2. SERIES COEFFICIENTS A_n

N_{Re}			42,647			
N_{Pr}	100	10	1.	0.1	0.01	
A_1	1.006	1.024	1.075	1.159	1.23	
A_2	−0.0094	−0.0357	−0.1117	−0.24	−0.3549	
A_3	0.00654	0.0194	0.06072	0.1388	0.2086	
A_4	−0.00769	−0.01497	−0.04337	−0.09859	−0.1465	
N_{Re}			11,695			
N_{Pr}	100	10	1.	0.1	0.01	
A_1	1.0063	1.026	1.089	1.179	1.239	
A_2	−0.01178	−0.04291	−0.1289	−0.2717	−0.3636	
A_3	0.01179	0.0272	0.0789	0.1606	0.207	
A_4	−0.01251	−0.02533	−0.05845	−0.1125	−0.1415	
N_{Re}			5,763			
N_{Pr}	100	10	1.	0.1	0.01	
A_1	1.0118	1.036	1.117	1.193	1.232	
A_2	−0.2143	−0.05069	−0.1672	−0.3022	−0.3408	
A_3	0.02277	0.04732	0.1015	0.1669	0.1874	
A_4	−0.01854	−0.0373	−0.07519	−0.1124	−0.124	
N_{Re}			5,038			4,800
N_{Pr}	100	10	1.	0.1	0.01	
A_1	1.018	1.059	1.141	1.205	1.217	1.201
A_2	−0.03668	−0.09756	−0.2188	−0.3051	−0.3232	−0.2992
A_3	0.03172	0.06999	0.13	0.1666	0.1729	0.1608
A_4	−0.02381	−0.05175	−0.09274	−0.1119	−0.1151	−0.1074

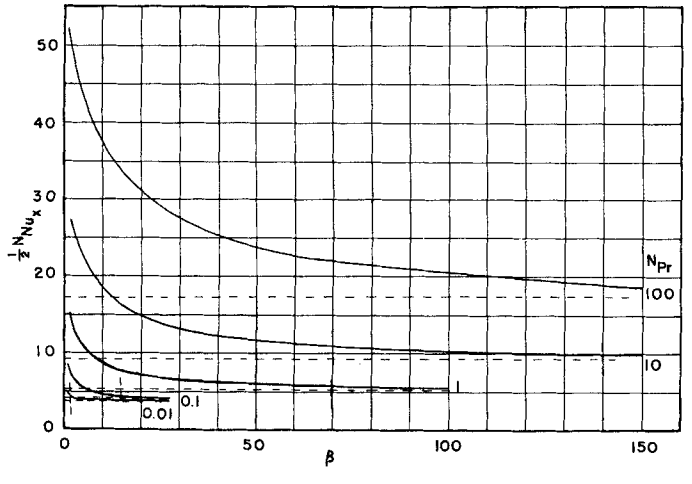

Fig. 2a. $N_{Re} = 5{,}038$.

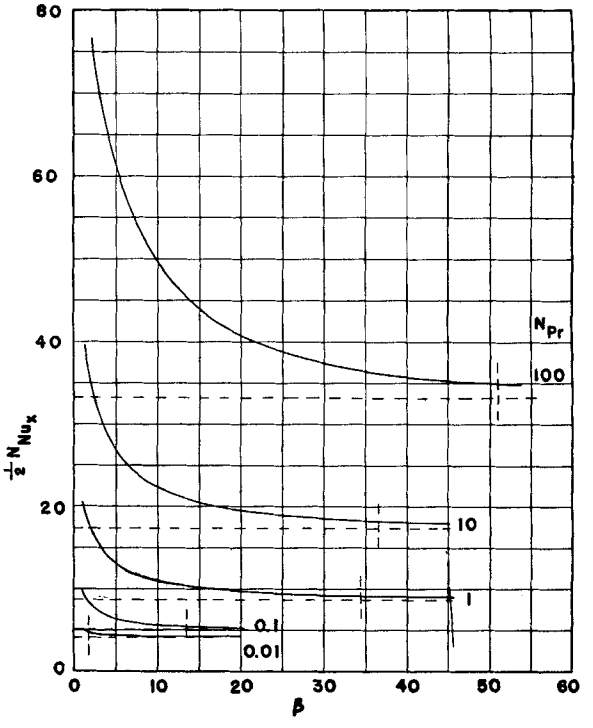

Fig. 2b. $N_{Re} = 5{,}763$.

Fig. 2. Nusselt number and thermal entrance length. Horizontal lines indicate asymptotic N_{Nu}. Vertical lines indicate the value of β at which $N_{Nu}/N_{Nu_\infty} = 1.05$.

The local N_{Nu} does not truly reflect the heat flux variation with distance from the inlet, since the bulk mean temperature varies as well. However the dimensionless temperature gradient at the wall is directly proportional to the heat flux. Therefore temperature gradients as a function of N_{Re} and N_{Pr} for $\beta = 5$ and $\beta = 25$ are given in Figures 4*a* and 4*b*. The temperature gradient at the wall, particularly at high, N_{Pr}, increases rapidly with increasing N_{Re}. If the gradient vs. β for various N_{Re} and N_{Pr} is plotted, it is found that at large β the curves flatten out showing that the resistance to heat transfer is fully established. As β decreases, the temperature gradient increases indicating a thinner effective thermal boundary layer and thus a larger quantity of heat transferred. In the case of highly conductive fluids, such as liquid metals, heat transferred in this region is of great practical importance, since equipment failures, which may occur due to thermal stress, can be disastrous.

The results of this investigation are also applicable to the case where the temperature distribution at the entrance is an arbitrary function of y, say $G(y)$. Clearly, this affects only Equation (5*a*). If say θ is defined in terms of the bulk mean inlet temperature, then one need modify only the A_n to

$$A_n = \frac{\int_0^1 \theta(0, \epsilon)\, U\, Y_n\, d\epsilon}{\int_0^1 U\, Y_n^2\, d\epsilon}$$

If the wall temperature is an arbitrary function of the axial distance, the method of superposition may be applied to the present results (9, 26).

It is relatively simple to test the validity of assumption 7 in an approximate way at least. To do this one may assume that total axial conduction is k times that radially. Hence Equation (2) becomes

$$UN_{Pe_m} \frac{\partial \theta}{\partial \beta} = \frac{\partial}{\partial \epsilon}\left(f \frac{\partial \theta}{\partial \epsilon}\right) + k \frac{\partial}{\partial \beta}\left(f \frac{\partial \theta}{\partial \beta}\right) \quad (18)$$

Let

$$\theta = \sum_{n=1}^{\infty} A_n F_n(\beta)\, Y_n(\epsilon) \quad (19)$$

where A_n and $Y_n(\epsilon)$ were previously determined. Substituting Equation (19) into (18) and integrating with respect

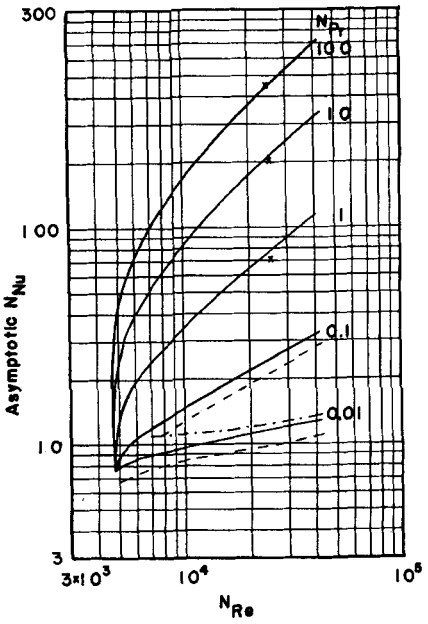

Fig. 3. Variation of asymptotic Nusselt number with Reynolds number for various N_{Pr}. *x*, — — — Gill and Sher (6); — . — . — . — . — Poppendiek (15).

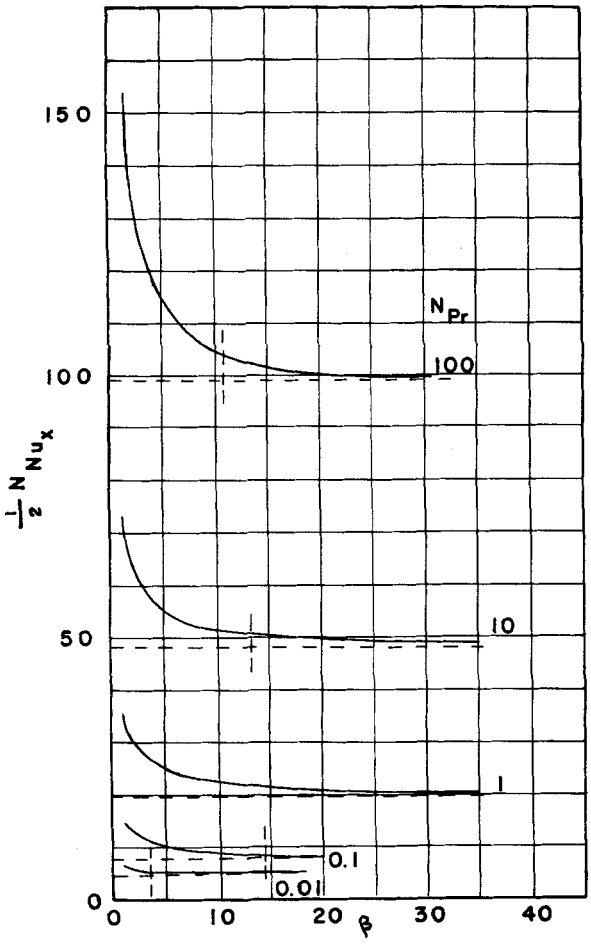

Fig. 2c. $N_{Re} = 11{,}695$.

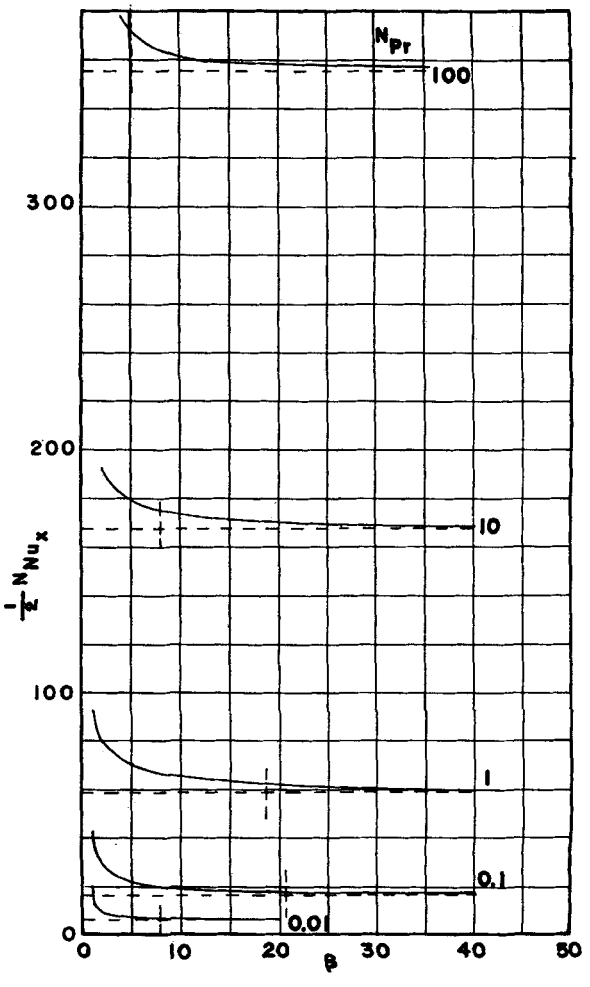

Fig. 2d. $N_{Re} = 42{,}647$.

Fig. 2. Nusselt number and thermal entrance length. Horizontal lines indicate asymptotic N_{Nu}. Vertical lines indicate the value of β at which $N_{Nu}/N_{Nu_\infty} = 1.05$.

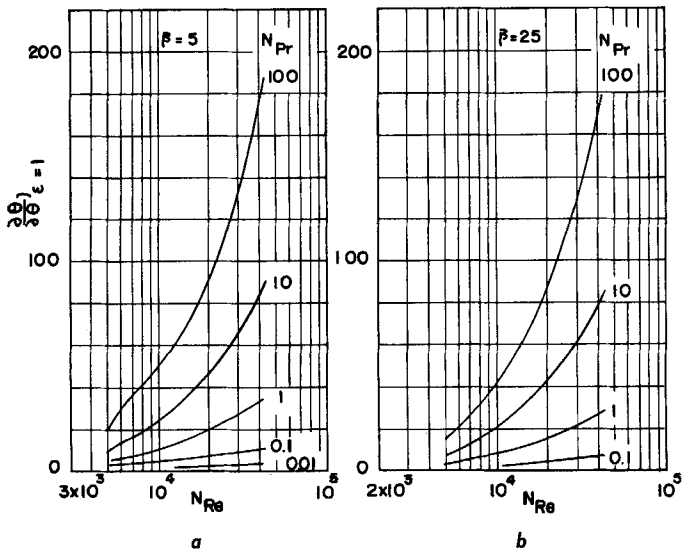

Fig. 4. Temperature gradient as a function of N_{Re} for various β.

to ϵ from 0 to 1 one obtains

$$\frac{d^2F_n}{d\beta^2} + \left[\frac{N_{Pe_m}\,Y_n'(1)}{k\,\lambda_n \int_o^1 f\,Y_n\,d\epsilon}\right]\frac{dF_n}{d\beta} + \frac{Y_n'(1)}{k\int_o^1 f\,Y_n\,d\epsilon}F_n = 0$$

Since $F_n(\infty) \to 0$

$$F_n(\beta) = e^{-\frac{N_{Pe_m}\,Y_n'(1)}{2\,k\,\lambda_n \int_o^1 f\,Y_n d\epsilon}\left[1-\sqrt{1-\frac{4\,k\,\lambda_n^2 \int_o^1 f\,Y_n d\epsilon}{N^2_{Pe_m}\,Y_n'(1)}}\right]\beta} \qquad (20)$$

The error introduced by assumption 7 can be estimated by comparing $(\lambda_n)/(N_{Pe_m})$ in Equation (5) with the corresponding term in the $F_n(\beta)$ functions. For the dominant initial terms in Equation (19) the value under the radical in Equation (20) is close to one, and hence it can be shown, with the binomial expansion, that the coefficients of β in the $F_n(\beta)$ functions differ from $(\lambda_n)/(N_{Pe_m})$ by less than

$$\frac{\lambda_n^3\,k\int_o^1 f\,Y_n\,d\epsilon}{4\,N^3_{Pe_m}\,Y_n'(1)}$$

For $N_{Pr} = 0.01$ and $N_{Re} = 5{,}038$, which is the worst condition studied, the error in the coefficient of β is approximately $(4k\,10^{-6})$ and $(2k\,10^{-3})$ for the first and second terms of the series respectively and is negligible for practical purposes.

The effects of dissipation, variation of the ratio ϵ_h/ϵ_m, variable properties of fluid, gravitational field effects, and unequal wall temperatures will be considered in future investigations concerning the transition region.

ACKNOWLEDGMENT

The computations were performed on the IBM-650 tape system of the Computing Center of Syracuse University and were in part supported by the National Science Foundation under grant NSF-G14594 awarded to the Computing Center. This work was supported in part by the office of Naval Research under contract NONR-669(17).

NOTATION

A = coefficient, Equation (5)
c_p = heat capacity (L^2/t^2T)
d = equivalent diameter (L)
f = $1 + \left(\frac{\epsilon_h}{\nu}\right) N_{Pr}$
F = friction factor (Fanning)
$G(y)$ = arbitrary initial temperature distribution
h = heat transfer coefficient (M/t^3T)
k = dimensionless constant equal to 0.36
K = thermal conductivity $\left(\frac{ML}{t^3T}\right)$
L = length (L)
M = mass (M)
r = distance from center to wall (L)
t = time (t)
T = temperature (T)
u = point velocity (L/t)
u^+ = dimensionless velocity parameter
u^* = friction velocity (L/t)
U = dimensionless velocity obtained by dividing any velocity by maximum velocity
x = axial distance (L)
y = distance from wall to center (L)
y^+ = dimensionless distance parameter (yu^*/ν)
Y = eigenfunction

Dimensionless Groups

N_{Nu} = Nusselt number $\left(\frac{4r_oh}{K}\right)$

Table 3. Derivatives of Eigenfunctions at the Wall

N_{Re}			42,647			
N_{Pr}	100	10	1.	0.1	0.01	
$Y'_1(1)$	−177.3	−82.01	−26.99	−6.792	−2.286	
$Y'_2(1)$	365	150	53.43	15.48	6.089	
$Y'_3(1)$	−730.2	−215.2	−74.31	−22.57	−9.597	
$Y'_4(1)$	1,626	299.8	96.04	29.24	12.95	
N_{Re}			11,695			
N_{Pr}	100	10	1.	0.1	0.01	
$Y'_1(1)$	−49.31	−23.55	−8.989	−3.127	−1.74	
$Y'_2(1)$	165.5	59.22	20.79	7.653	4.77	
$Y'_3(1)$	−480.2	−105.1	−31.93	−11.67	−7.508	
$Y'_4(1)$	854.7	155.7	41.66	15.27	10.03	
N_{Re}			5,763			
N_{Pr}	100	10	1.	0.1	0.01	
$Y'_1(1)$	−16.52	−8.365	−3.788	−1.928	−1.554	
$Y'_2(1)$	119	29.3	10.02	5.019	4.166	
$Y'_3(1)$	−270.5	−58.04	−15.17	−7.511	−6.349	
$Y'_4(1)$	303.7	72.5	20.51	9.809	8.332	
N_{Re}			5,038			4,800
N_{Pr}	100	10	1.	0.1	0.01	
$Y'_1(1)$	−8.488	−4.387	−2.265	−1.586	−1.483	−1.429
$Y'_2(1)$	71.42	17.49	6.337	4.172	3.899	3.807
$Y'_3(1)$	−102.4	−27.14	−9.472	−6.374	−6.002	−5.92
$Y'_4(1)$	122.9	33.42	12.21	8.43	7.97	7.893

N_{Pe_m} = (N_{Re_m}) (N_{Pr})

N_{Pr} = Prandtl number $\left(\frac{c_p\mu}{K}\right)$

N_{Re} = Reynolds number $\left(\frac{4r_o u_b}{\nu}\right)$

N_{Re_m} = $\frac{r_o u_m}{\nu}$

Greek Letters

α = thermal diffusivity $\left(\frac{K}{c_p\rho}\right)$

β = dimensionless axial distance $\left(\frac{x}{r_o}\right)$

ϵ_h = eddy diffusivity of heat (L^2/t)

ϵ_m = eddy diffusivity of momentum (L^2/t)

ϵ = dimensionless distance from center to wall $\left(\frac{r}{r_o}\right)$

θ = dimensionless temperature $\left(\frac{T-T_o}{T_i-T_o}\right)$

λ = eigenvalue

μ = viscosity (M/Lt)

ν = kinematic viscosity (L^2/t)

ρ = density (M/L^3)

σ = $\int_o^\epsilon \frac{d\epsilon}{f}$

Subscripts

b = mean value

i = inlet value

l = index

m = maximum value

n = mode of eigenvalue

o = wall value

∞ = asymptotic value

LITERATURE CITED

1. Beckers, H. L., *Appl. Sci. Res.*, **A6**, 147 (1956).
2. Beskin, L., and R. M. Rosenberg, *J. Aeronaut. Sci.*, **13**, 597 (1946).
3. Brown, G. M., *A.I.Ch.E. Journal*, **6**, 179 (1960).
4. Deissler, R. G., *Natl. Advisory Comm. Aeronaut. Rept. 1210* (1955).
5. ———, *Natl. Advisory Comm. Aeronaut. Tech. Note 2629* (1952).
6. Gill, W. N., and Marvin Scher, *J. Chem. Eng. Data*, **6**, 347 (1961).
7. Gill, W. N., *Appl. Sci. Res.*, **A11**, 10 (1962).
8. ———, and Marvin Scher, *A.I.Ch.E. Journal*, **7**, 61 (1961).
9. Hildbrand, F. B., "Advanced Calculus for Engineering," Prentice-Hall, Englewood Cliffs, New Jersey (1958).
10. Lin, G. S., R. W. Moulton, and G. L. Putnam, *Ind. Eng. Chem.*, **45**, 636 (1953).
11. Martinelli, R. C., *Trans. Am. Soc. Mech. Engrs.*, **69**, 947 (1947).
12. Meksyn, D., "New Methods in Laminar Boundary-Layer Theory," Chap. 20, Pergamon Press, New York (1961).
13. Mickley, H. S., T. K. Sherwood, and C. E. Reed, "Applied Mathematics in Chemical Engineering," p. 254, McGraw-Hill, New York (1957).
14. Murphree, E. V., *Ind. Eng. Chem.*, **24**, 726 (1932).
15. Poppendiek, H. F., *Natl. Aeronaut Space Administration MEMO 2-5-59w* (1959).
16. Prandtl, L., *Z. Physik*, **11**, 1072 (1910); **29**, 487 (1928).
17. Reichardt, H., *Nat'l. Advisory Comm. Aeronaut. Tech. Memo 1047* (1943).
18. Reynolds, O., *Proc. Manchester Literary Philosophical Soc.*, **8**, (1874).
19. Rothfus, R. R., and D. E. Baldwin, *A.I.Ch.E. Journal*, **7**, 352 (1961).
20. Seban, R. A., and T. T. Shimazaki, *Trans. Am. Soc. Mech. Engrs.*, **73**, 803 (1951).
21. Senecal, V. E., Ph.D. thesis, Carnegie Inst. Technol., Pittsburgh, Pennsylvania (1952).
22. Sleicher C. A., *Trans. Am. Soc. Mech. Engrs.*, **79**, 789 (1957).
23. Sparrow, E. M., T. M. Hallman, and R. Siegel, *Appl. Sci. Res.*, **A7**, 37 (1957).
24. Taylor, G. I., *Adv. Comm. Aeronaut. (Great Britain) Tech. Rept. 272* (1916).
25. Temple, G., and W. G. Bickley, "Rayleigh's Principle," Oxford Univ. Press, New York (1933).
26. Tribus, M., and J. Klein, "Heat Transfer Symposium," Univ. Michigan, Ann Arbor, Michigan (1952).
27. Von Karman, Theodore, *Trans. Am. Soc. Mech. Engrs.*, **61**, 705 (1939).
28. Whan, G. A., and R. R. Rothfus, *A.I.Ch.E. Journal*, **5**, 204 (1959).

Manuscript received September 11, 1961; revision received November 8, 1961; paper accepted November 17, 1961.

Mass Transfer and Effective Interfacial Areas in Packed Columns

FUMITAKE YOSHIDA and TETSUSHI KOYANAGI

Kyoto University, Kyoto, Japan

Experimental studies on the mass transfer rates were performed for three kinds of operations: vaporization of water into air; absorption of methanol vapor by water; and distillation of three binary mixtures, trichloroethylene-toluene, ethanol-water, and acetone-water, by use of columns of the same diameter packed with 25- and 15-mm. Raschig rings. Correlations are presented for the individual phase height of a transfer unit and also for the effective interfacial areas. The effective areas for a given packing vary depending on the kind of operation as well as on the liquid rate and surface tension. The effective interfacial area for vaporization is significantly larger than that for absorption. The effective area for distillation seems to be roughly the same as that for absorption, if correction is made for the effect of surface tension.

Separation of volumetric mass transfer coefficients in packed columns, such as k_Oa and k_La, into the mass transfer coefficient, k_G or k_L, and the effective interfacial area a was attempted by Shulman and co-workers (*22*) and by the present authors (*30*). However there remains a question of whether or not the effective area varies with the kind of operation. This paper compares the effective areas for vaporization and absorption and presents the results of a study on a packed distillation column. Columns of the same diameter were used throughout the three kinds of experiments.

Tetsushi Koyanagi is at Kansai University, Osaka, Japan.